

1 **First evidence for multiple-harmonic standing Alfvén**  
2 **waves in Jupiter’s equatorial plasma sheet**

3 **H. Manners<sup>1</sup>, A. Masters<sup>1</sup>**

4 <sup>1</sup>Space and Atmospheric Physics Group, Blackett Laboratory, Imperial College London, London, UK

5 **Key Points:**

- 6 • We report first evidence of several simultaneous wave harmonics on the same mag-  
7 netic field line in Jupiter’s plasma sheet.
- 8 • The harmonic periods, elliptical polarization, and confinement to the plasma sheet  
9 all agree with predictions for standing Alfvén waves.
- 10 • Multiple-harmonic standing Alfvén waves could explain the entire range of quasi-  
11 periodic pulsations observed in Jupiter’s magnetosphere.

---

Corresponding author: Harry Manners, [h.manners17@imperial.ac.uk](mailto:h.manners17@imperial.ac.uk)

## Abstract

Quasi-periodic pulsations in the ultra-low-frequency band are ubiquitously observed in the jovian magnetosphere, but their source and distribution have until now been a mystery. Standing Alfvén waves on magnetic field lines have been proposed to explain these pulsations and their large range in observed periods. However, in-situ evidence in support of this mechanism has been scarce. Here we use magnetometer data from the Galileo spacecraft to report first evidence of a multiple-harmonic ultra-low-frequency event in Jupiters equatorial plasma sheet. The harmonic periods lie in the 4-22-min range, and the nodal structure is confined to the plasma sheet. Polarization analysis reveals several elliptically-polarized odd harmonics, and no presence of even harmonics. The harmonic periods, their polarization, and the confinement of the wave to the plasma sheet, are strong evidence supporting the standing Alfvén wave model. Multiple-harmonic waves therefore potentially explain the full range of periods in quasi-periodic pulsations in Jupiters magnetosphere.

## 1 Introduction

Unexplained quasi-periodic (QP) pulsations in the ultra-low-frequency (ULF) band have been observed throughout the jovian magnetosphere since Pioneer 10 first encountered the system in 1973 (Kivelson, 1976). Jupiter’s enormous magnetosphere is capable of supporting waves of far lower frequency than the terrestrial magnetospheric ULF spectrum, and so the label ULF is often extended to  $< 1\text{mHz}$ . Observations span multiple datasets, most predominately X-Ray, IR and UV auroral emission modulations (Gladstone et al., 2002; Nichols et al., 2017; Dunn et al., 2017; Watanabe et al., 2018), magnetic perturbations (Khurana & Kivelson, 1989), radio emissions (MacDowall et al., 1993; Hospodarsky et al., 2004; Arkhypov & Rucker, 2006; Kimura et al., 2011, 2012) and energetic particle flux modulations (Anagnostopoulos et al., 2001; Karanikola et al., 2004). The combined range of observed periods spans 1-100+ minutes, with several preferential 15-minutes, 30-minutes and 40-minutes periods referred to as QP15, QP30 and QP40, respectively. The topic has been well reviewed recently by Delamere (2016). Several studies have attempted to assess ULF wave activity in the middle magnetosphere, and found significant wave power within 1-100-minutes, but none spanned the full range (Khurana & Kivelson, 1989; Tsurutani et al., 1993; Schulz et al., 1993; Petkaki & Dougherty, 2001; Wilson & Dougherty, 2000; Russell et al., 2001). Most of these studies looked for trav-

44 elling ULF waves (with the exception of the standing wave description in Khurana and  
45 Kivelson (1989), however Voyager 2 moved too rapidly to resolve harmonic structures).  
46 Ultimately, determining the cause of these pulsations has proven challenging. At the time  
47 of writing, whether they are the result of a single mechanism or several is yet to be con-  
48 firmed.

49 Despite these difficulties, it is clear that perturbations should correlate between datasets  
50 in a system as highly coupled as a planetary magnetosphere. Any local departure from  
51 equilibrium in a magnetosphere creates Alfvén waves, which carry field-aligned currents  
52 (FACs). These FACs propagate along the field lines towards the ionospheric footprints  
53 and modulate the local current density and particle distributions, which are responsi-  
54 ble for polar-region electromagnetic emissions. The evidence supports this connection,  
55 and seems to be most prevalent in the middle magnetosphere: quasi-periodic ULF mag-  
56 netic perturbations in the middle magnetosphere have strong Alfvénic components (Khurana  
57 & Kivelson, 1989), and pulsations in the auroral emissions are often in regions where the  
58 magnetic field lines map to the middle magnetosphere (Gladstone et al., 2002; Nichols  
59 et al., 2017). The pulsations are therefore likely the result of a single mechanism per-  
60 turbing the magnetic field that subsequently modulates other observables, exhibiting the  
61 same range of periods. As ULF periods  $\gtrsim 10$ -mins correspond to wavelengths compara-  
62 ble to the size of the magnetospheric cavity, these pulsations are consistent with a global  
63 Alfvénic resonance of the magnetic field.

64 A well-established literature exists regarding magnetospheric resonance and ULF  
65 waves in the terrestrial magnetosphere (see Takahashi et al. (2006) for a detailed overview).  
66 It has been shown that ULF waves have an important role in the flow of energy and mo-  
67 mentum through the terrestrial magnetosphere, and in understanding phenomena such  
68 as diffusive transport of electrons, radiation belt dynamics, ionospheric particle precip-  
69 itation, and myriad wave-particle interactions. These behaviours result from trapping  
70 wave energy at low-frequencies (corresponding to large scales) on a finite timescale, pro-  
71 viding free energy to smaller-scale processes after an initial disturbance has ceased, of-  
72 ten far from the site of disturbance. Without analogous knowledge of ULF waves in the  
73 jovian magnetosphere a full understanding of magnetospheric dynamics cannot be ex-  
74 pected.

75 The presiding paradigm in terrestrial magnetospheric literature claims that ULF  
76 waves can be explained by the field-line-resonance (FLR) mechanism. In this descrip-

77 tion, Kelvin-Helmholtz (KH) vortices or other large-scale perturbations on the magne-  
78 topause are advected around the flanks of the magnetopause and produce evanescent,  
79 circularly-polarized fast-mode MHD waves that propagate into the magnetosphere, as  
80 outlined in Chen and Hasegawa (1974). In regions of inhomogeneity, the fast-mode waves  
81 can couple to the Alfvénic MHD mode and drive standing Alfvén waves on magnetic field  
82 lines analogous to vibrating strings (D. Southwood, 1974). The plasma sheet in the jo-  
83 vian magnetosphere is a region of significant inhomogeneity, and so the fast and Alfvénic  
84 modes should be strongly coupled, therefore a mechanism analogous to the field-line-resonance  
85 mechanism may be active. However, it is unclear how the established literature for ter-  
86 restrial magnetospheric resonance translates to the magnetospheres of the outer plan-  
87 ets (though comparisons have been made of the ULF wave activity between planets, e.g.  
88 Glassmeier (1995)). In addition to standing Alfvén waves, travelling fast-mode wave en-  
89 ergy may be trapped locally by a cavity resonance mode. It has been shown that cav-  
90 ity resonances in the terrestrial magnetosphere provide a persistent source of energy to  
91 slowly build large amplitude standing Alfvén waves (Kivelson & Southwood, 1985). In  
92 the terrestrial magnetosphere the most notable cavity mode is between the magnetopause  
93 and the plasmopause. The jovian magnetosphere is suffused with plasma everywhere and  
94 so lacks a plasmopause, and the geometric distortion the field due to the plasma sheet  
95 makes an analogous cavity mode unlikely. However, the equatorial plasma density gra-  
96 dient potentially makes the plasma sheet boundaries reflective. This could create res-  
97 onant cavities inside the plasma sheet, or between the ionosphere and plasma sheet bound-  
98 ary as suggested by Nichols et al. (2017). In either case the mode would probably be more  
99 accurately described as a wave-guide, because the wave energy is likely to be eventually  
100 lost down-tail (McPherron, 2005). As the majority of pulsation observations have been  
101 associated with Alfvénic activity, we focus on trans-hemispheric standing Alfvén waves  
102 as our primary candidate mechanism. A series of studies have built on the early work  
103 of D. Southwood (1974); Chen and Hasegawa (1974) and D. Southwood and Hughes (1982)  
104 to develop a magnetospheric box-model of standing Alfvén waves in the jovian magne-  
105 tosphere (D. J. Southwood & Kivelson, 1986; Kivelson & Southwood, 1986; Khurana &  
106 Kivelson, 1989). A key difference in the jovian model from equivalent terrestrial mod-  
107 els is the effect of the jovian equatorial plasma sheet. As the plasma density in the plasma  
108 sheet is orders of magnitude higher than in the higher-latitude regions (lobes), the Alfvén  
109 travel time is dominated by the plasma sheet thickness and Alfvén speed (see Fig. 27

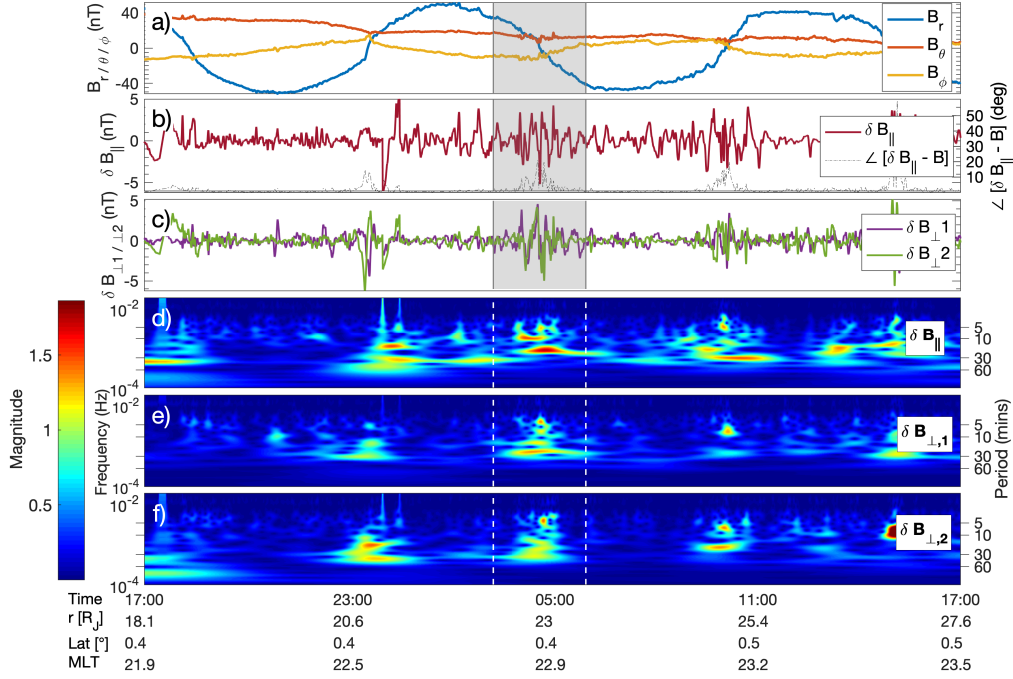
110 in Bagenal et al. (2017)). Conservation of energy flux of also means that the magnetic  
 111 perturbation amplitude is maximised inside the plasma sheet. The combination of these  
 112 effects results in the MHD wave power and standing wave nodal structure being effec-  
 113 tively confined to the equatorial region. Recently, Manners et al. (2018) used the box  
 114 model first presented by Kivelson and Southwood (1986) to compare standing Alfvén wave  
 115 eigenperiods to all of the QP ULF periods observed at Jupiter. They found that either  
 116 due to either spatial variation in plasma sheet properties, or a superposition of harmon-  
 117 ics on the same field line, standing Alfvén waves are consistent with the full range of ob-  
 118 servations. We can therefore explain all ULF pulsations in the jovian magnetosphere with  
 119 a single mechanism. However, further analysis has been hindered by the lack of clearly  
 120 resolved in-situ observations.

121 Here we present the first evidence for multiple harmonics of a standing Alfvén wave  
 122 on the same field line, confined inside the equatorial plasma sheet. In section 2 we present  
 123 an algorithm searching for ULF waves using magnetometer data from the Galileo space-  
 124 craft. In section 3 we present a multiple-harmonic standing Alfvén wave discovered by  
 125 our algorithm. In section 4 we discuss the implications multiple-harmonics may have for  
 126 explaining the wide range of reported ULF periods.

## 127 **2 Searching for Ultra-Low-Frequency Waves in Jupiter’s Magnetosphere**

128 We used data from the Galileo spacecraft (Kivelson et al., 1992), which followed  
 129 an equatorial trajectory for the majority of its 34 orbits, in the vicinity of Jupiter’s equa-  
 130 torial plasma sheet and the surrounding lobes. Galileo traversed the magnetic equator  
 131 thousands of times, due to the spacecraft’s equatorial orbit, Jupiter’s 10-hour rotational  
 132 period and the  $\sim 10^\circ$  obliquity of the planet’s dipole. Unfortunately, Galileo suffered  
 133 damage that meant data from all instruments had to be transmitted to Earth at a decimated  
 134 bit-rate. Additionally, the Plasma Science (PLS) instrument suffered damage to the elec-  
 135 trostatic analyzers (Bagenal et al., 2016). Low cadence and pointing constraints make  
 136 the ion moments of limited use for this survey (see supplementary material for details).  
 137 Here we use only the magnetometer data to search for magnetic perturbations close to  
 138 the plasma sheet.

147 The magnetic perturbation fields of interest are typically of order  $\sim 1$  nT. To in-  
 148 spect these small-amplitude perturbations, we rotated the data into the mean-field-aligned  
 149 (MFA) coordinate system outlined in Manners et al. (2018), which uses a sliding aver-



139 **Figure 1.** Magnetometer data from the Galileo spacecraft during 7th-8th November 1996,  
 140 centred on a multiple-harmonic standing Alfvén wave. The event is highlighted by the grey  
 141 blocks or vertical dashed white lines in each panel. a) Magnetic field data in spherical system  
 142 III coordinates. b) Compressional component of the mean-field-aligned (MFA) magnetic field  
 143 residual (red line), and the deviation angle between the local magnetic field vector and the MFA  
 144 unit vectors (black dashed line). c) Both transverse components of the MFA magnetic field resid-  
 145 ual. d-f) Continuous wavelet transforms for the compressional and Alfvénic MFA magnetic field  
 146 residuals, respectively.

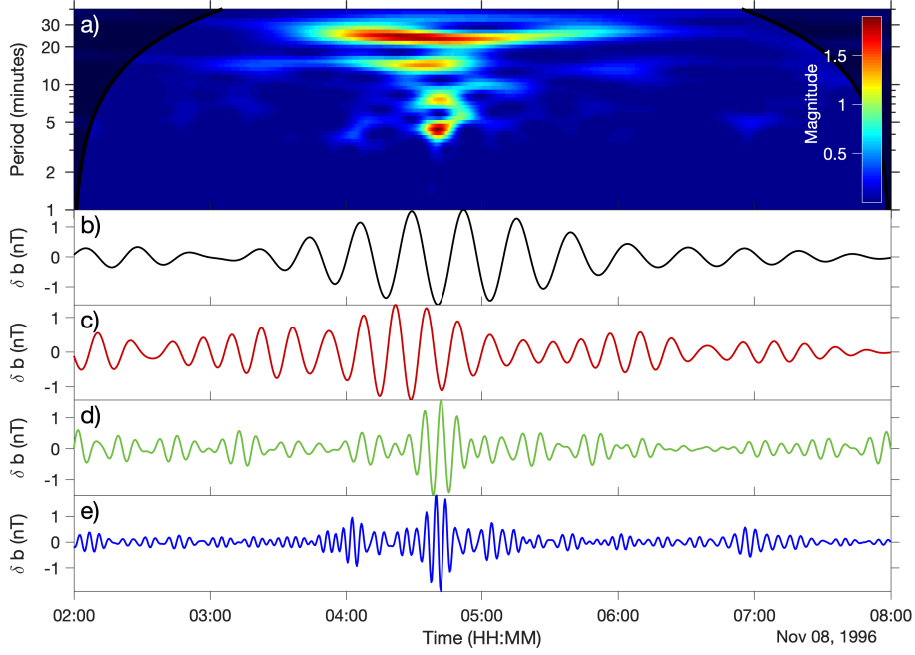
150 age window of width 60-mins to produce a principal unit vector  $\hat{b}_{||}$  aligned with the av-  
 151 erage background magnetic field. The unit vectors  $\hat{b}_{\perp,1}$  and  $\hat{b}_{\perp,2}$  complete the right-handed  
 152 orthogonal set and are transverse to the mean field. The rotated field components can  
 153 then be detrended using the sliding average obtained during the rotation, giving the mean-  
 154 field-aligned residual magnetic field components  $\delta b_{||}$ ,  $\delta b_{\perp,1}$  and  $\delta b_{\perp,2}$ . In regions where  
 155 the background field is stable on the timescale of the sliding window, the quasi-perpendicular  
 156 MFA components isolate Alfvénic MHD wave activity. However, regions of high variabil-  
 157 ity such as the middle magnetosphere the background field changes significantly within  
 158 the width of the sliding window, producing residuals comparable to the magnitude of

159 the predicted ULF wave signatures. This means that signals detected beyond  $\sim 30R_J$   
 160 cannot be distinguished from short-timescale change in the background magnetic field.  
 161 Conversely, at radii inside Io's orbit and the inside edge of the plasma torus ( $\sim 5R_J$ )  
 162 the latitudinal plasma density gradient is more shallow, and so the Alfvén travel time  
 163 is on the order of seconds (see Fig. 27 in Bagenal et al. (2017)), and so is not a region  
 164 of interest. However, in the region  $\sim 10\text{--}30R_J$  there exists a coherent equatorial body  
 165 of high-density plasma, and the plasma swept past Galileo on a timescale  $>1$ -hour, pro-  
 166 ducing residuals in the MFA components of  $< 0.1$  nT, much smaller than the wave sig-  
 167 natures of interest. This is also the region where the time taken to transit the plasma  
 168 sheet is maximised, and so is the ideal region to obtain the greatest coverage of events.

169 We identified many events of interest in the MFA residuals, which spanned the ULF  
 170 frequency band and showed significant broadband wave power or coincident wave power  
 171 maxima at discrete frequencies. For the remainder of this study we present and anal-  
 172 yse the best resolved event, measured by Galileo on 8th November, 1996. The data and  
 173 MFA residuals are shown in Figure 1 a)-c). At this time, Galileo was travelling through  
 174 the midnight sector in the middle magnetosphere, at a radial distance from Jupiter of  
 175  $\sim 20\text{--}30R_J$ . To obtain details of the MFA residuals in frequency-time space, we com-  
 176 puted the continuous wavelet transforms (CWTs) of each MFA residual component. The  
 177 results are shown in Figure 1 d)-f). We assumed a Morlet wavelet to perform the com-  
 178 putation, and the cone-of-influence (COI) regions, where edge effects dominate, lie be-  
 179 yond the limits of the axes. Maxima in wavelet power are evident in all three perturba-  
 180 tion components between periods of  $\sim 5\text{--}25$  minutes, several of which are coincident,  
 181 especially in  $\delta\vec{b}_{\perp,1}$ . These coincident wavelet power maxima are noticeably separated into  
 182 discrete frequency bands in the components transverse to the field, indicating Alfvénic  
 183 activity at several ULF frequencies simultaneously. To properly identify the event we anal-  
 184 ysed its structure and polarization.

### 185 **3 A Multiple-Harmonic Ultra-Low-Frequency Pulsation during 8th Novem-** 186 **ber 1996**

187 We concentrate on the first transverse MFA component,  $\delta b_{\perp,1}$ , because it shows  
 188 well-resolved coincident wave power maxima. Figure 2 a) shows a magnified view of the  
 189 CWT of  $\delta b_{\perp,1}$  during the pulsation at around 4:45AM (highlighted by the grey region  
 190 in Figure 1). Integrating the wavelet power over the pulsation interval, we find four dis-  
 191 tinct maxima at  $\sim 22$  minutes,  $\sim 14$  minutes,  $\sim 7$  minutes and  $\sim 4$  minutes. The ratios be-



195 **Figure 2.** Processed data from the first Alfvénic MFA magnetic residual component,  $\delta b_{\perp,1}$ . a)  
 196 Continuous wavelet transform of  $\delta b_{\perp,1}$  during the event highlighted in Figure 1 (COI represented  
 197 by black envelope). Four coincident wave power maxima are evident at the perturbation maxi-  
 198 mum, at around 4:45AM. b)-e) Band-pass filtered time series of  $\delta b_{\perp,1}$  for the wave power maxima  
 199 at  $\sim 22$  minutes,  $\sim 14$  minutes,  $\sim 7$  minutes and  $\sim 4$  minutes, respectively.

192 tween consecutive maxima are close to 2, indicative of a harmonic series. These results  
 193 are insensitive to the frequency analysis method used, as confirmed by fast-Fourier trans-  
 194 form and Lomb-Scargle analyses (see supplementary materials).

200 We isolate each period by taking the full-width-half-maximum (FWHM) of Gaus-  
 201 sians fitted to each peak in the integrated wavelet power. Performing band-pass filters  
 202 of the MFA residual time series, we obtain the decomposed time series for each peak in  
 203 wavelet power, shown in Figure 2 b)-e). Each filtered time series shows a clear wave-packet  
 204 structure at the pulsation maximum. The same filtering routine was applied to  $\delta b_{\parallel}$  and  
 205  $\delta b_{\perp,2}$ , with similar results.

206 The wave periods and restriction of the wave to the quasi-Alfvénic plane are in-  
 207 sufficient to determine whether the event is the result of a superposition of travelling per-  
 208 turbations or a standing wave structure. However, theoretical treatment of standing Alfvén  
 209 waves, e.g. Chen and Hasegawa (1974); D. Southwood (1974), predict that the wave po-



210 larization in the plane transverse to the magnetic field reverses over a magnetic pertur-  
 211 bation maximum (plasma displacement node). We can therefore determine whether the  
 212 event has a standing profile by inspecting its polarization in the field-transverse plane.

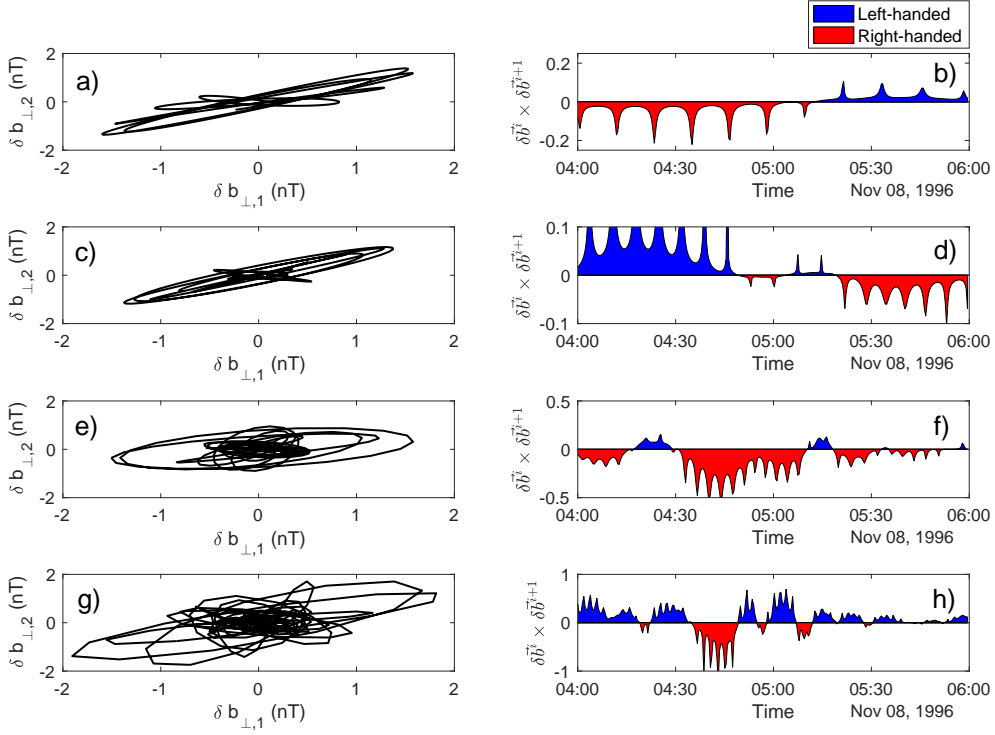
219 Figure 3 a), c), e) and g) show hodograms for the 22-min, 14-min, 7-min and 4-min  
 220 signals, respectively, revealing them all to be elliptically polarized. Panels b), d), f) and  
 221 h) show the unit vector in the direction normal to the plane created by the cross-product  
 222 between transverse components of each consecutive pair of MFA magnetic field resid-  
 223 ual vectors,  $\delta\vec{b}^i = (0, \delta b_{\perp,1}^i, \delta b_{\perp,2}^i)$  and  $\delta\vec{b}^{i+1} = (0, \delta b_{\perp,1}^{i+1}, \delta b_{\perp,2}^{i+1})$ . This normal vector  
 224 reverses sign when the lead/lag of the two transverse components is also reversed, cor-  
 225 responding to changes in handedness of the polarization. By counting the number of nodes,  
 226 we can determine the wave harmonic number. Using the hodograms and normal vectors  
 227 in conjunction, we find that each signal is an elliptically polarized odd harmonic. More  
 228 reversals could exist outside the plasma sheet region, but those visible in the data pro-  
 229 vide a lower limit.

#### 230 **4 First Evidence for Multiple-Harmonic Standing Alfvén Waves in Jupiter’s** 231 **Plasma Sheet**

232 Thus far we have shown several key features of the ULF pulsation centred  $\sim 4:45$ AM  
 233 on 8th November 1996: multiple discrete periods with each successive period doubling,  
 234 confinement of the wave to the plasma sheet, and a reversal in handedness over the am-  
 235 plitude maxima. Combined, these features are in strong support of an equatorially-confined  
 236 standing Alfvén wave on a single magnetic field line, with multiple harmonics excited  
 237 simultaneously.

238 To compare the decomposed signals with predicted standing Alfvén wave harmon-  
 239 ics, we refer to a magnetospheric box model previously adapted for the jovian magne-  
 240 tosphere (D. J. Southwood & Kivelson, 1986; Khurana & Kivelson, 1989; Manners et al.,  
 241 2018). As each field line acts as a linear resonator with an independent set of harmonic  
 242 periods, the model uses a 1D model field-line to solve for the field-line eigenperiods, parametrized  
 243 by the Alfvén speed inside the plasma sheet, and the sheet half-thickness.

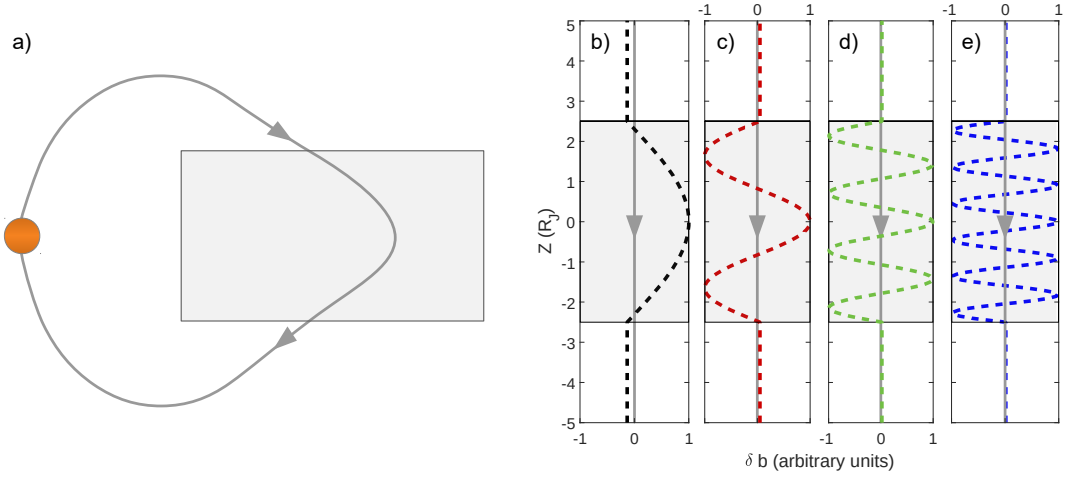
252 Figure 4 shows the magnetic field perturbation eigenfunctions, for the 1st, 3rd, 7th  
 253 and 11th harmonics, obtained from the box model. For demonstrative purposes, we chose  
 254 parameters to emphasize the equatorial confinement of the nodes by assuming a nom-  
 255 inal plasma sheet half-thickness of  $2.5 R_J$ , an equatorial Alfvén speed of 100 km/s, and  
 256 a high-latitude Alfvén speed of  $3.5 \times 10^4$  km/s (based on Fig. 27 of Bagenal et al. (2017)).



213 **Figure 3.** a), c), e), g) Hodograms of the bandpass-filtered time series for the 22 min, 14  
 214 min, 7, min and 4 min signal, showing distinct elliptical polarization. b), d), f), h) The corre-  
 215 sponding vector cross-product of consecutive MFA magnetic residual vectors  $\delta \vec{b}^i \times \delta \vec{b}^{i+1}$ , where  
 216  $\delta \vec{b}^i = \left( 0, \delta b_{\perp,1}^i, \delta b_{\perp,2}^i \right)$  for  $i \in \{0, T - 1\}$ , where  $T$  is the total time during the interval. This  
 217 produces time series for  $\hat{n} \sin \theta$ , where  $\hat{n}$  gives the direction of the normal unit vector to the plane  
 218 formed by consecutive MFA magnetic residual vectors, and  $\theta$  is the angle between them.

257 Though the exact number of nodes in the 7-min and 4-min periods is difficult to deter-  
 258 mine, the number of nodes is odd, and so the depicted harmonics in Figure 4 give an ac-  
 259 curate qualitative description. Periods consistent our observations can be produced by  
 260 a degenerate combination of plasma sheet parameters, as shown by Fig. 4 in Manners  
 261 et al. (2018). If jovian magnetospheric dynamics are conducive to exciting multiple har-  
 262 monics of standing Alfvén waves on the same field line, the large range in QP ULF pe-  
 263 riods could arise not only from spatial variation of plasma sheet properties, but also due  
 264 to a spectrum of harmonics generated on each field line, or a combination of both.

265 Inspecting Figure 1, the harmonic structure in  $\delta b_{\perp,2}$  is not as well-defined as in  $\delta b_{\perp,1}$ .  
 266 This could arise from the imperfect alignment of the MFA coordinate system, or the asym-



244 **Figure 4.** a) Cartoon of a typical magnetic field line (solid grey line) mapping from Jupiter  
 245 (orange circle) out to the middle jovian magnetosphere at  $\sim 23R_J$ . The radial distension of the  
 246 magnetic field is visible, especially inside the equatorial plasma sheet (light grey rectangles).  
 247 b)-e) The black, red, green and blue dashed lines depict solutions of the magnetic perturbation  
 248 eigenfunctions for the 1st, 3rd, 7th and 11th harmonics obtained from the magnetospheric box  
 249 model developed by D. J. Southwood and Kivelson (1986). The eigenfunctions are plotted as a  
 250 function of displacement along the field line from the magnetic equator,  $Z$ . The nominal field line  
 251 is shown by the solid grey lines.

267 metry could indicate that a strict plane-wave approximation is insufficient. Alternatively,  
 268 it could be evidence of decoupled poloidal and toroidal resonance modes. In the vicin-  
 269 ity of the plasma sheet in the middle magnetosphere, the MFA coordinate system pro-  
 270 duces a  $\delta b_{\perp,1}$  that is quasi-toroidal, and  $\delta b_{\perp,2}$  that is quasi-poloidal. As  $\delta b_{\perp,1}$  contains  
 271 most of the wave power, the event periods could be evidence for a toroidal standing Alfvén  
 272 wave.

273 The absence of even harmonics is equally significant. Modelling indicates that suc-  
 274 cessive even and odd harmonics should be excited. The absence of even harmonics may  
 275 be a signature of the driving mechanism. In the literature concerning terrestrial mag-  
 276 netospheric ULF waves, the excitation of standing Alfvén waves is thought to arise from  
 277 both internal and external drivers (Oimatsu et al., 2018). Several internal mechanisms  
 278 have been proposed, such as the bounce, drift-mirror and drift-bounce resonances (D. South-  
 279 wood et al., 1969; Hughes et al., 1978; Khurana & Kivelson, 1989; Hasegawa & Chen,  
 280 2013). The drift-bounce resonance, however, is asymmetric about the magnetic equa-

281 tor, and the wavelengths involved in the drift-mirror instability are too small to match  
 282 the observed ULF wave periods.

283 The observation critical to confirming a KH-driven FLR mechanism is the pres-  
 284 ence of a circularly-polarised travelling fast-mode wave. However, a standing Alfvén wave  
 285 would persist for some time after the travelling wave front had passed. If the resonance  
 286 is not critically damped, would persist for several wave periods, which indicates a po-  
 287 tential lifetime for the wave from several hours to tens of hours. The actual character-  
 288 istic lifetime is dependent on the dominant damping mechanism in the jovian magne-  
 289 tosphere, consideration of which is beyond the remit of this study. We speculate that  
 290 the compressional component periods in  $\delta b_{\parallel}$  represent such a cavity resonance confined  
 291 between the plasma sheet boundaries, feeding energy into a multiple harmonics of a stand-  
 292 ing Alfvén wave on a single field line.

293 It is worth noting that we found no significant wave power with periods above 22  
 294 minutes. The absence of a 40-min periodicity (QP-40) commonly observed in the jovian  
 295 magnetosphere is curious. Though the significance of this cannot be determined from  
 296 a single event, we speculate that that QP-40 is characteristic of a region of the magne-  
 297 tosphere not encountered during this event, or is globally the most commonly excited  
 298 resonant period.

## 299 5 Summary

300 We surveyed magnetometer data from the Galileo spacecraft during its orbital tour  
 301 of the jovian magnetosphere, looking for quasi-periodic ultra-low-frequency pulsations.  
 302 We presented a single event confined to inside the equatorial plasma sheet. Polarization  
 303 analysis revealed several elliptically polarized odd harmonics in the plane quasi-transverse  
 304 to the mean field. These data represent the first observation of a multiple-harmonic stand-  
 305 ing Alfvén wave in Jupiter’s equatorial plasma sheet, consistent with predictions by (Manners  
 306 et al., 2018).

307 We showed that, in addition to spatial variation in properties of the equatorial plasma  
 308 sheet producing a range in resonant periods, each resonant field line is capable of gen-  
 309 erating periodic pulsations across the full range of ULF periods. We showed that the event  
 310 we analysed had a distinct absence of even modes. We have no explanation for this ab-  
 311 sence, but we speculate that it is highly relevant to determining the driving mechanism.

312 Several more events similar to the one we present here exist in the Galileo dataset.  
 313 More work remains to be done regarding the possible resonance modes of the complex  
 314 jovian magnetospheric geometry, and the driving mechanisms responsible for exciting  
 315 them. The multiple-harmonic standing Alfvén wave we have presented here changes the  
 316 current picture of sporadic ULF waves at Jupiter, indicative at least of a semi-permanent  
 317 population of multiple-harmonic standing Alfvén waves on field lines throughout the mag-  
 318 netosphere. In future studies we will assess the spatial distribution of pulsations in the  
 319 jovian equatorial plasma sheet, and their respective harmonic structure.

### 320 **Acknowledgments**

321 Harry Manners is supported by a Royal Society PhD Studentship. Adam Masters is sup-  
 322 ported by a Royal Society University Research Fellowship. Data required to reproduce  
 323 the results shown can be obtained from the NASA Planetary Data System (<https://pds.nasa.gov>).  
 324 Please direct correspondence to Harry Manners ([h.manners17@ic.ac.uk](mailto:h.manners17@ic.ac.uk)).

### 325 **References**

- 326 Anagnostopoulos, G., Aggelis, A., Karanikola, I., & Marhavilas, P. (2001). Energetic  
 327 ion (>50keV) and electron (>40keV) bursts observed by Ulysses near Jupiter.  
 328 *Adv. Sp. Res.*, *28*(6), 903–908. doi: 10.1016/S0273-1177(01)00514-2
- 329 Arkhypov, O. V., & Rucker, H. O. (2006). Ultra low frequencies phenomena in Jo-  
 330 vian decametric radio emission. *Astron. Astrophys.*, *452*(1), 347–350. doi: 10  
 331 .1051/0004-6361:20054334
- 332 Bagenal, F., Adriani, A., Allegrini, F., Bolton, S. J., Bonfond, B., Bunce, E. J., . . .  
 333 Zarka, P. (2017). Magnetospheric Science Objectives of the Juno Mission.  
 334 *Space Sci. Rev.*, *213*(1-4), 219–287. doi: 10.1007/s11214-014-0036-8
- 335 Bagenal, F., Wilson, R. J., Siler, S., Paterson, W. R., & Kurth, W. S. (2016). Sur-  
 336 vey of Galileo plasma observations in Jupiter’s plasma sheet. *J. Geophys. Res.*  
 337 *Planets*, *121*(5), 871–894. doi: 10.1002/2016JE005009
- 338 Chen, L., & Hasegawa, A. (1974). A theory of long-period magnetic pulsations: 1.  
 339 Steady state excitation of field line resonance. *J. Geophys. Res.*, *79*(7), 1024–  
 340 1032. doi: 10.1029/JA079i007p01024
- 341 Delamere, P. A. (2016). A Review of the Low-Frequency Waves in the Gi-  
 342 ant Magnetospheres. *Low-Frequency Waves Sp. Plasmas*, 365–378. doi:

343 10.1002/9781119055006.ch21

344 Dunn, W. R., Branduardi-Raymont, G., Ray, L. C., Jackman, C. M., Kraft, R. P.,  
 345 Elsner, R. F., ... Coates, A. J. (2017). The independent pulsations of Jupiter's  
 346 northern and southern X-ray auroras. *Nat. Astron.*, *1*(11), 758–764. doi:  
 347 10.1038/s41550-017-0262-6

348 Gladstone, G. R., Waite, J. H., Grodent, D., Lewis, W. S., Crary, F. J., Eisner,  
 349 R. F., ... Cravens, T. E. (2002). A pulsating auroral X-ray hot spot on  
 350 Jupiter. *Nature*, *415*(6875), 1000–1003. doi: 10.1038/4151000a

351 Glassmeier, K.-H. (1995). Ultralow-frequency pulsations: Earth and Jupiter com-  
 352 pared. *Adv. Sp. Res.*, *16*(4), 209–218. doi: 10.1016/0273-1177(95)00232-4

353 Hasegawa, A., & Chen, L. (2013). Theory of the Drift Mirror Instability. In (pp.  
 354 173–177). doi: 10.1029/GM053p0173

355 Hospodarsky, G. B., Kurth, W. S., Cecconi, B., Gurnett, D. A., Kaiser, M. L.,  
 356 Desch, M. D., & Zarka, P. (2004). Simultaneous observations of Jovian quasi-  
 357 periodic radio emissions by the Galileo and Cassini spacecraft. *J. Geophys.*  
 358 *Res. Sp. Phys.*, *109*(A9), 1–13. doi: 10.1029/2003JA010263

359 Hughes, W. J., Southwood, D. J., Mauk, B., McPherron, R. L., & N., B. J. (1978).  
 360 Alfvén waves generated by an inverted plasma energy distribution. *Nature*,  
 361 *275*(5675), 43–45. doi: 10.1038/275043a0

362 Karanikola, I., Athanasiou, M., Anagnostopoulos, G. C., Pavlos, G. P., & Preka-  
 363 Papadema, P. (2004). Quasi-periodic emissions (15- 80 min ) from the poles  
 364 of Jupiter as a principal source of the large-scale high-latitude magnetopause  
 365 boundary layer of energetic particle. *Planet. Space Sci.*, *52*(5-6), 543–559. doi:  
 366 10.1016/j.pss.2003.10.002

367 Khurana, K. K., & Kivelson, M. G. (1989). Ultralow frequency MHD waves in  
 368 Jupiter's middle magnetosphere. *J. Geophys. Res.*, *94*(A5), 5241. doi: 10.1029/  
 369 JA094iA05p05241

370 Kimura, T., Cecconi, B., Zarka, P., Kasaba, Y., Tsuchiya, F., Misawa, H., &  
 371 Morioka, A. (2012). Polarization and direction of arrival of Jovian quasiperi-  
 372 odic bursts observed by Cassini. *J. Geophys. Res. Sp. Phys.*, *117*(11), 1–15.  
 373 doi: 10.1029/2012JA017506

374 Kimura, T., Tsuchiya, F., Misawa, H., Morioka, A., & Nozawa, H. (2010). Occur-  
 375 rence statistics and ray tracing study of Jovian quasiperiodic radio bursts

- 376 observed from low latitudes. *J. Geophys. Res. Phys.*, *115*(5), n/a. doi:  
 377 10.1029/2009JA014647
- 378 Kimura, T., Tsuchiya, F., Misawa, H., Morioka, A., Nozawa, H., & Fujimoto, M.  
 379 (2011). Periodicity analysis of Jovian quasi-periodic radio bursts based on  
 380 Lomb-Scargle periodograms. *J. Geophys. Res. Sp. Phys.*, *116*(3), 1–10. doi:  
 381 10.1029/2010JA016076
- 382 Kivelson, M. G. (1976). Jupiter's Distant Environment. In D. Williams (Ed.), *Phys.*  
 383 *sol. planet. environ. proc. int. symp. solar-terrestrial phys.* (Volume 2 ed., pp.  
 384 836–853). Washington D.C.: Physics of solar planetary environments. doi:  
 385 10.1029/SP008p0836
- 386 Kivelson, M. G., Khurana, K. K., Means, J. D., Russell, C. T., & Snare, R. C.  
 387 (1992). The Galileo magnetic field investigation. *Space Sci. Rev.*, *60*(1-4),  
 388 357–383. doi: 10.1007/BF00216862
- 389 Kivelson, M. G., & Southwood, D. J. (1985). Resonant ULF waves: A new interpre-  
 390 tation. *Geophys. Res. Lett.*, *12*(1), 49–52. doi: 10.1029/GL012i001p00049
- 391 Kivelson, M. G., & Southwood, D. J. (1986). Coupling of global magnetospheric  
 392 MHD eigenmodes to field line resonances. *J. Geophys. Res.*, *91*(A4), 4345. doi:  
 393 10.1029/JA091iA04p04345
- 394 MacDowall, R. J., Kaiser, M. L., Desch, M. D., Farrell, W. M., Hess, R. A., & Stone,  
 395 R. G. (1993). Quasiperiodic Jovian Radio bursts: observations from the  
 396 Ulysses Radio and Plasma Wave Experiment. *Planet. Space Sci.*, *41*(11-12),  
 397 1059–1072. doi: 10.1016/0032-0633(93)90109-F
- 398 Manners, H., Masters, A., & Yates, J. N. (2018). Standing Alfvén Waves in Jupiter's  
 399 Magnetosphere as a Source of 10- to 60-Min Quasiperiodic Pulsations. *Geo-*  
 400 *phys. Res. Lett.*, *45*(17), 8746–8754. doi: 10.1029/2018GL078891
- 401 McPherron, R. L. (2005). Magnetic pulsations: Their sources and relation to solar  
 402 wind and geomagnetic activity. *Surv. Geophys.*, *26*(5), 545–592. doi: 10.1007/  
 403 s10712-005-1758-7
- 404 Nichols, J. D., Yeoman, T. K., Bunce, E. J., Chowdhury, M. N., Cowley, S. W. H., &  
 405 Robinson, T. R. (2017). Periodic emission within Jupiter's main auroral oval.  
 406 *Geophys. Res. Lett.* doi: 10.1002/2017GL074824
- 407 Oimatsu, S., Nosé, M., Teramoto, M., Yamamoto, K., Matsuoka, A., Kasahara,  
 408 S., ... Lindqvist, P.-A. (2018). Drift-Bounce Resonance Between Pc5

- 409 Pulsations and Ions at Multiple Energies in the Nightside Magnetosphere:  
410 Arase and MMS Observations. *Geophys. Res. Lett.*, 45(15), 7277–7286. doi:  
411 10.1029/2018GL078961
- 412 Petkaki, P., & Dougherty, M. K. (2001). ULF wave observations in Jupiter’s magne-  
413 tosphere. *Adv. Sp. Res.*, 28(6), 909–914. doi: 10.1016/S0273-1177(01)00517-8
- 414 Russell, C. T., Blanco-Cano, X., & Strangeway, R. J. (2001). Ultra-low-frequency  
415 waves in the Jovian magnetosphere: Causes and consequences. *Planet. Space*  
416 *Sci.*, 49(3-4), 291–301. doi: 10.1016/S0032-0633(00)00150-1
- 417 Schulz, M., Blake, J., Mazuk, S. M., Balogh, A., Dougherty, M. K., Forsyth, R. J.,  
418 ... Bame, S. J. (1993). Energetic particle, plasma and magnetic field signa-  
419 tures of a poloidal pulsation in Jupiter’s magnetosphere. *Planet. Space Sci.*,  
420 41(11-12), 967–975. doi: 10.1016/0032-0633(93)90101-7
- 421 Southwood, D. (1974). Some features of field line resonances in the magnetosphere.  
422 *Planet. Space Sci.*, 22(3), 483–491. doi: 10.1016/0032-0633(74)90078-6
- 423 Southwood, D., Dungey, J., & Etherington, R. (1969). Bounce resonant interaction  
424 between pulsations and trapped particles. *Planet. Space Sci.*, 17(3), 349–361.  
425 doi: 10.1016/0032-0633(69)90068-3
- 426 Southwood, D., & Hughes, W. (1982). Theory of Hydromagnetic Waves in the Mag-  
427 netosphere. *Space Sci. Rev.*, 35, 301–366.
- 428 Southwood, D. J., & Kivelson, M. G. (1986). The effect of parallel inhomogeneity on  
429 magnetospheric hydromagnetic wave coupling. *J. Geophys. Res.*, 91(A6), 6871.  
430 doi: 10.1029/JA091iA06p06871
- 431 Takahashi, K., Chi, P. J., Denton, R. E., & Lysak, R. L. (Eds.). (2006). *Magneto-*  
432 *spheric ULF Waves: Synthesis and New Directions* (Vol. 169). Washington, D.  
433 C.: American Geophysical Union. doi: 10.1029/GM169
- 434 Tsurutani, B. T., Southwood, D. J., Smith, E. J., & Balogh, A. (1993). A Survey  
435 of Low Frequency Waves at Jupiter: The Ulysses Encounter. *J. Geophys. Res.*,  
436 98(A12), 21203–21216. doi: 10.1029/93JA02586
- 437 Watanabe, H., Kita, H., Tao, C., Kagitani, M., Sakanoi, T., & Kasaba, Y. (2018).  
438 Pulsation Characteristics of Jovian Infrared Northern Aurora Observed by  
439 the Subaru IRCS with Adaptive Optics. *Geophys. Res. Lett.*, 547–554. doi:  
440 10.1029/2018GL079411
- 441 Wilson, R. J., & Dougherty, M. K. (2000). Evidence provided by galileo of ultra low



442 frequency waves within Jupiter's middle magnetosphere. *Geophys. Res. Lett.*,  
443 27(6), 835–838. doi: 10.1029/1999GL006070